Available online at www.sciencedirect.com
ScienceDirect
Ceramics International 35 (2009) 1581–1586
CERAMICS INTERNATIONAL
www.elsevier.com/locate/ceramint

TiO_2 nanoceramic films prepared by ion beam assisted evaporation for optical application

Su-Shia Lin [a,*], Shin-Chi Chen [b], Yuan-Hsun Hung [b]

[a] Department of Applied Materials and Optoelectronic Engineering, National Chi Nan University, Puli, Nantou Hsien 54561, Taiwan, ROC
[b] Institute of Mechatronoptic Systems, Chienkuo Technology University, Changhua 500, Taiwan, ROC

Received 26 June 2008; received in revised form 1 August 2008; accepted 28 August 2008
Available online 8 October 2008

Abstract

A TiO_2 nanoceramic film was prepared as an alternative absorber layer for infrared thermal detectors. The TiO_2 film was amorphous, and its grain size increased with the ion anode voltage and oxygen flow rate. Moiré deflectometry was applied for measuring the nonlinear refractive indices of TiO_2 films on polycarbonate (PC) substrates. The nonlinear refraction index was measured to be of the order of 10^{-8} cm^2 W^{-1} and the change in refractive index was of the order of 10^{-5}. The linear refractive index was correlated with the porosity. Denser TiO_2 films exhibited higher linear refractive indices, obvious red-shifts and narrower absorption bands in the near-IR region.

Keywords: Film; Refractive index; Porosity; Absorption

1. Introduction

Uncooled thermal imaging system made of thin film materials has numerous military and civilian applications. The infrared detectors made of ferroelectric thin film are heated by radiation and release electric-charges because of the pyroelectricity of the material. A black layer is usually grown on the top electrode of a ferroelectric detector to maximize absorption of radiation within the spectral bands of interest. Among the numerous oxide materials, titanium dioxide (TiO_2) has received interest due to its superior physical, chemical properties and high stability. In this study, an infrared-absorber layer composed of TiO_2 nanoceramic film was deposited by ion beam assisted evaporation. This deposition technique is well established to produce dense and adhesive optical films.

Titanium dioxide has three phases in nature—anatase, rutile and brookite. Amorphous TiO_2 thin films are formed at low substrate temperatures [1–5]. Structural changes may occur during the heating process [2]. Such structural changes lead to complications for optical characterization and the quality control of TiO_2 films [6–10]. Therefore, the substrate was not heated in this study. Polycarbonate (PC) was selected as the substrate material for coating TiO_2 films, because of its good impact strength and high transparency. The structure and properties of TiO_2 thin films depend strongly on processing technique. The influence of experimental conditions (mainly the ion anode voltage and oxygen flow rate) on the properties of TiO_2 films was investigated.

Transparent materials generally exhibit the optical Kerr effect. The nonlinear refractive indices of materials are of great interest because of potential applications in designing optical devices [11–14]. Moiré deflectometry is a powerful tool for measuring the nonlinear refractive indices of materials. The main advantages of the Moiré deflectometry technique are its extreme experimental simplicity, lower cost and lower sensitivity to external disturbances than those of other interferometric methods. In this study, this method was applied to measure the nonlinear refractive indices of TiO_2 films on PC substrates under illumination with a 5-mW He–Ne laser ($\lambda = 632.8$ nm).

2. Experimental procedures

The TiO_2 nanoceramic films were deposited on PC substrate by ion beam assisted evaporation. The source material was TiO_2 powder (99.99% purity, UENO Taito-Ku, Tokyo, Japan).

* Corresponding author. Tel.: +886 49 2910960x4771; fax: +886 49 2912238.
E-mail address: sushia@ncnu.edu.tw (S.-S. Lin).

0272-8842/$34.00
doi:10.1016/j.ceramint.2008.08.022

The diameter of powder was in the range of 1–3 mm. The PC substrates were ultrasonically cleaned in alcohol, rinsed in deionized water, and subsequently dried in flowing nitrogen gas before deposition.

The evaporation was performed in Ar–O_2 atmosphere with the source material-to-substrate distance of 12 cm. A cryo-pump coupled with a rotary pump was used to achieve an ultimate pressure of 8.7×10^{-5} Pa before introducing argon gas (99.99%, Lien Hwa Gas Co., Hsin Chu, Taiwan). For the TiO_2 nanoceramic layer deposition, the substrate was not heated. The chamber was back-filled with Ar–O_2 at a working pressure of 5.3×10^{-2} Pa. The TiO_2 powders were put in a water-cooled crucible. To accelerate the electrons, the filament cathode assembly potential was biased negatively with respect to a nearby grounded anode by anywhere at 6 V. In addition, a transverse magnetic field was applied to deflect the electron beam in a 270° circular arc and focused it on the hearth and evaporant charge at ground potential. The power was maintained at 1.0 kW. The thickness of TiO_2 films was maintained at 80 nm. The ion anode voltage was in the range of 90–120 eV. The oxygen flow rate was in the range of 1–3 sccm.

The film thickness was measured using a surface profiler (Alpha-Sep 500, TENCOR, USA) and a FE-SEM (XL-40FEG Field Emission Scanning Electron Microscope, Netherlands). An X-ray diffractometer (XRD) (Rigaku D/MAX2500, Japan) was used to study the structure of the films. The X-ray source was a sealed Cu Kα (λ = 1.5418 Å). The surface morphologies of the TiO_2 films were examined by atomic force microscopy (AFM; Digital Instruments Inc., NanoScope E, USA). The optical absorption spectra of films in the vis–IR region were recorded by a spectrophotometer (TRIAX 180/190; TRIAX Series Spectrometers, France). The linear refractive indices of films were recorded using a spectrometer (ST4000-200, Korea).

The Moiré deflectometry experimental set-up used to measure the nonlinear refractive indices of TiO_2 films on PC substrates is shown in Fig. 1. A 5-mW He–Ne laser beam (wavelength of 632.8 nm) was focused by lens L_1 and is re-collimated by lens L_2. The focal lengths of lenses L_1 and L_2 are 100 and 200 mm, respectively. Two similar Ranchi gratings G_1 and G_2 with pitch of 0.1 mm were used to construct the Moiré fringes patterns. The distance between planes of G_1 and G_2 is chosen 64 mm and it was known as one of Talbot distances for the used gratings. The Talbot distances are characterized by $z_t = tp^2/\lambda$where, p is the periodicity of the grating, λ is the wavelength of light and t is an integer. In this work, the Moiré fringes were clearly formed for Talbot distance of $z_{t=4} \approx 64$ mm. This means that the Moiré fringes were observed on a screen attached to the second grating. The Moiré fringes patterns were projected on a computerized CCD camera by lens L_3, placed at the back of the second grating.

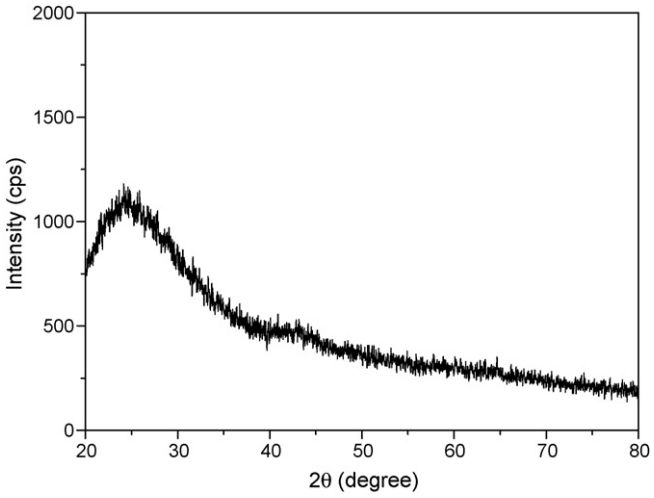

Fig. 2. The X-ray diffraction pattern of TiO_2 film prepared at an ion anode voltage of 110 eV and the oxygen flow rate of 3 sccm.

3. Results and discussion

3.1. Structural characterization

Fig. 2 shows the X-ray diffraction pattern of TiO_2 film prepared at an ion anode voltage of 110 eV and the oxygen flow rate of 3 sccm. No long-range order was observed from the X-ray diffraction pattern of TiO_2 film, corresponding to an amorphous layer. The TiO_2 films have a structure with only short-range order or regions where the atoms are predictably placed. However, within a very few atom spacing, this order breaks down, and no long-range correlation is in the geometric positioning of the atoms.

Fig. 3 shows the 2D AFM images of TiO_2 films deposited under different conditions. In Fig. 3a, the TiO_2 films were composed of irregular grains with grain size of 30–60 nm, and included only a few pores. According to Fig. 3a and b, the average grain size increased with the ion anode voltage. At high ion anode voltage, the kinetic energies of the particles were high, and the grains were larger. By comparing Fig. 3b and c,

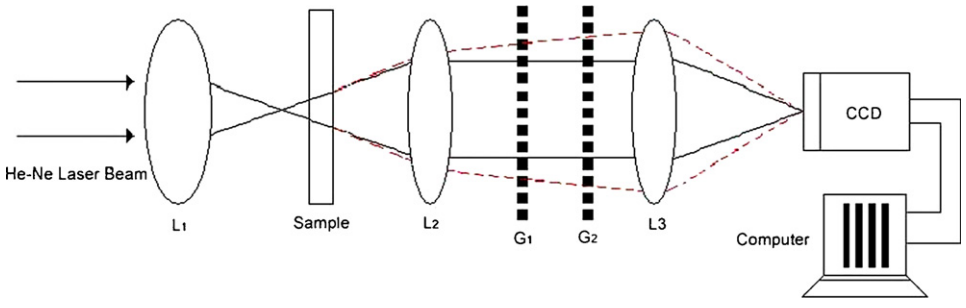

Fig. 1. The experimental set-up for measuring index of nonlinear refraction by Moiré deflectometry technique.

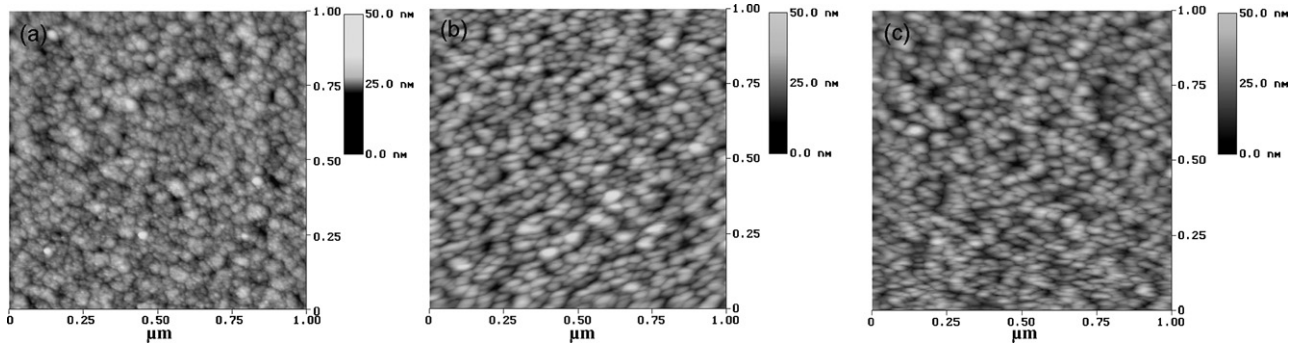

Fig. 3. The 2D AFM images of TiO_2 films prepared at different conditions. The ion anode voltage and the oxygen flow rate are: (a) 90 eV, 3 sccm; (b) 110 eV, 3 sccm; and (c) 110 eV, 1 sccm.

there were few pores existing in the TiO_2 films prepared at 3 sccm. The probability of collisions of particles increased with increasing oxygen atmosphere, it is probably why TiO_2 nanoceramic films prepared at oxygen flow rate of 3 sccm showed few pores.

Fig. 4 shows the scanning electron micrograph of the cross-section for TiO_2 films prepared at an ion anode voltage of 110 eV and the oxygen flow rate of 3 sccm. It could be observed that the TiO_2 films developed a dense structure. TiO_2 films prepared under different conditions also show the similar results.

3.2. Optical properties

The index of refraction, n, which depends on the radiation intensity, may be expressed in terms of nonlinear index n_2 ($cm^2\ W^{-1}$):

$$n(r,z) = n_0 + n_2 I(r,z) = n_0 + \Delta n(r,z) \tag{1}$$

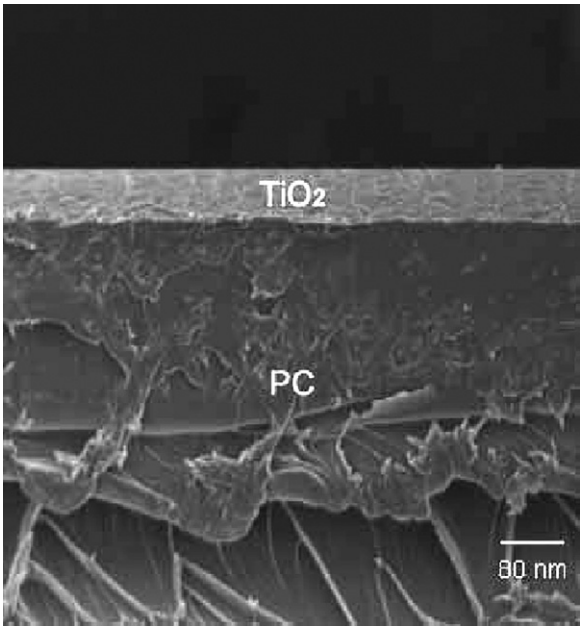

Fig. 4. The scanning electron micrograph of the cross-section for TiO_2 films prepared at an ion anode voltage of 110 eV and the oxygen flow rate of 3 sccm.

where n_0 is the linear index of refraction; $I(r, z)$ is the irradiance of the laser beam within the sample and $\Delta n(r, z)$ is the light-induced refractive index change. Based on the assumption that a Gaussian beam is traveling in the $+z$ direction, the beam irradiance can be written as

$$I(r,z) = I_0 \frac{\omega_0^2}{\omega^2(z)} \exp\left[-\frac{2r^2}{\omega^2(z)}\right] \tag{2}$$

where r is the radial radius of imaginational sphere; ω_0 is the spot size of the beam at the focus; $\omega(z) = \omega_0(1 + z^2/z_0^2)^{1/2}$ is the beam radius at a distance z from the position of the waist, $z_0 = \pi\omega_0^2/\lambda$ is the diffraction length of the Gaussian beam, and λ is the wavelength. The irradiance of the beam at the focus is denoted I_0 and in terms of the input laser power, p_{in}, equals $2p_{in}/\pi\omega_0^2$. Therefore, for a Gaussian laser beam, the radial dependence of the irradiance gives rise to a radially dependent parabolic refractive index change near the beam axis:

$$\Delta n(r,z) = n_2 I_0 \frac{\omega_0^2}{\omega^2(z)} \exp\left[-\frac{2r^2}{\omega^2(z)}\right]. \tag{3}$$

Moiré deflectometry is a sensitive technique for measuring changes in the refractive indices of materials. The sensitivity of this technique is determined by the minimum angle of rotation (α_{min}) that can be measured. Fig. 5 shows the Moiré fringe rotation angle versus z for the TiO_2 film on PC substrate. The TiO_2 film was prepared at an ion anode voltage of 110 eV and the oxygen flow rate of 3 sccm. The tested sample was placed at various distances from the focal point of lens L_1. The minimum rotation angle was obtained from the figure. The same experiment was performed using the pure PC substrate alone to check the contribution of PC substrate in the nonlinear refraction measurement. The result showed no observed fringes rotations or change in fringe size.

For the thin nonlinear medium of thickness d, the lowest nonlinear refractive index can be written as

$$n_{2,min} = \frac{\theta f_2^2}{z_t} \frac{\pi\omega_0^4}{d\, p_{in} z_0^2} \alpha_{min} \tag{4}$$

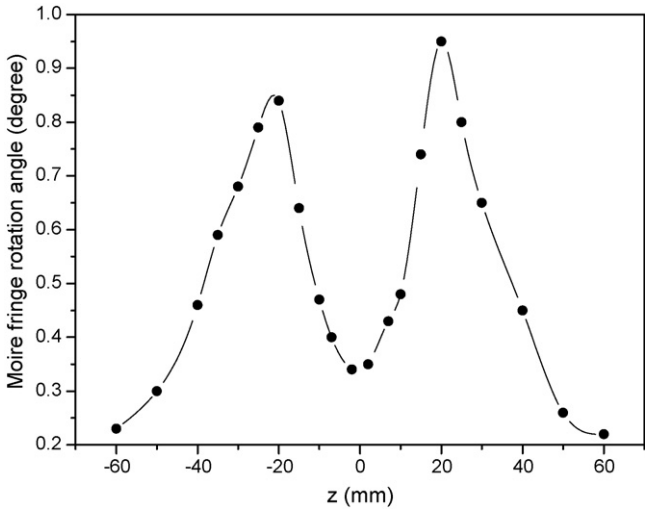

Fig. 5. The Moiré fringe rotation angle versus z for the TiO_2 film on PC substrate.

and the change in minimum refractive index is

$$\Delta n_{\min} = \frac{\omega_0^2 \theta f_2^2}{2 d z_t z_0^2} \alpha_{\min}. \quad (5)$$

The nonlinear refraction index was measured to be of the order of 10^{-8} cm^2 W^{-1} and the change in refractive index was of the order of 10^{-5}.

Fig. 6 shows the Moiré fringe patterns of the TiO_2 films that were deposited on PC substrates under different conditions. According to Fig. 6a–c, the Moiré fringes exhibited no rotation or change in size, suggesting that the increasing the ion anode voltage and oxygen flow rate did not obviously change the number of pores.

Fig. 7 shows the linear refractive index and the porosity of TiO_2 films prepared at (a) different ion anode voltages and (b) different oxygen flow rates. The linear refractive index n_0 was measured at a wavelength of 632.8 nm. In Fig. 7a, the TiO_2 films were prepared at the oxygen flow rate of 3 sccm and the different ion anode voltages. The linear refractive index of TiO_2 film increased with the ion anode voltage. An amorphous structure has a lower refractive index than pure anatase. In this study, TiO_2 films were amorphous layers. Therefore, the linear refractive index is directly correlated with the porosity [15].

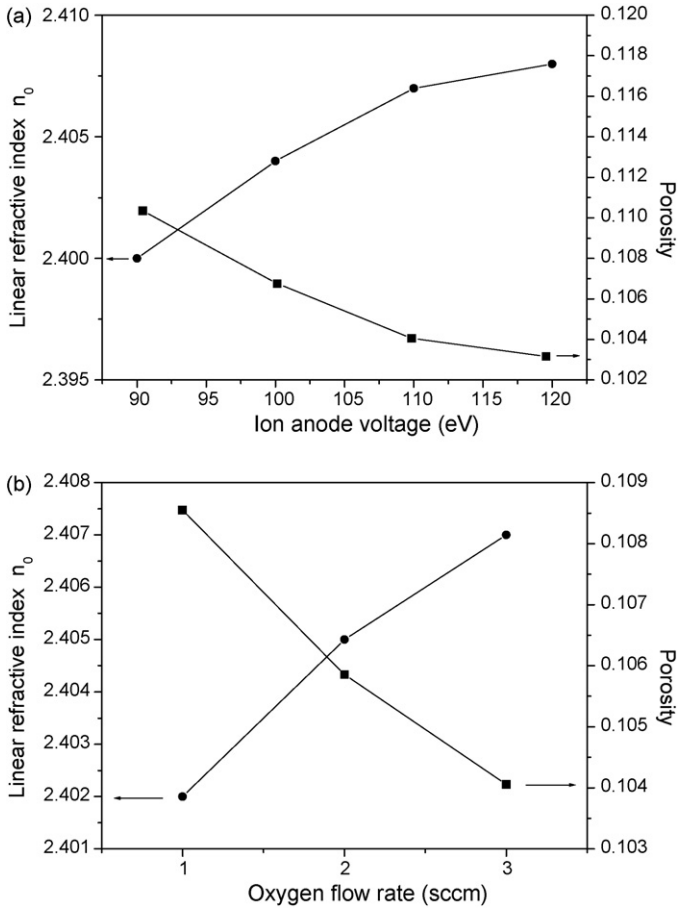

Fig. 7. The linear refractive index and the porosity of TiO_2 films prepared at (a) different ion anode voltages and (b) different oxygen flow rates.

If the film is assumed to be composed of pure anatase, then the porosity can be estimated using the following equation [16]:

$$\text{porosity} = 1 - \frac{n_0^2 - 1}{n_a^2 - 1} \quad (6)$$

where n_0 is the linear refractive index of the porous coating film and n_a is the linear refractive index of dense anatase TiO_2 film (2.52) found in the literature [17]. The porosity values are only useful for comparing with those obtained by other authors, because of the use of the refractive index of pure anatase noted as n_a is an oversimplification [15]. The porosity of TiO_2 film

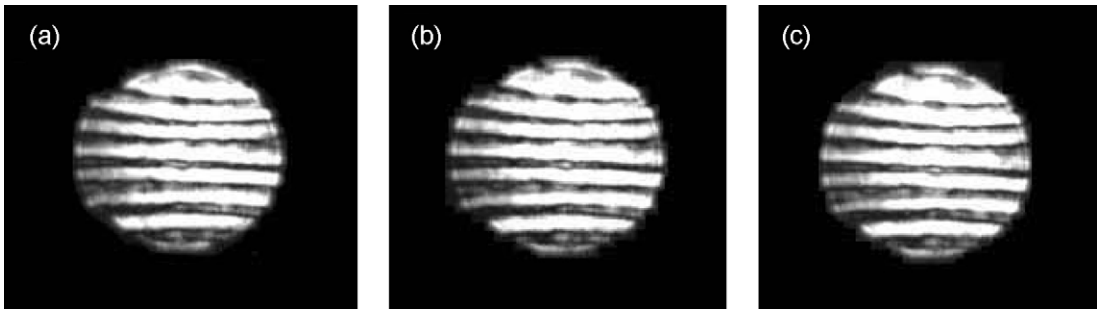

Fig. 6. The Moiré fringe patterns of the TiO_2 films that were deposited on PC substrates under different conditions. The ion anode voltage and the oxygen flow rate are: (a) 90 eV, 3 sccm; (b) 110 eV, 3 sccm; and (c) 110 eV, 1 sccm.

decreased as the ion anode voltage increased, but not much. This result is in good agreement with Fig. 3.

In Fig. 7b, the TiO_2 films were prepared at an ion anode voltage of 110 eV and different oxygen flow rates. As the oxygen flow rate increased, the linear refractive index increased, but the porosity decreased. It indicated that the dense TiO_2 film with a high linear refractive index could be obtained by increasing the oxygen flow rate.

Fig. 8 shows the absorbance in the vis–IR region of TiO_2 films prepared at (a) different ion anode voltages and (b) different oxygen flow rates. In Fig. 8a and b, the spectra were not symmetrical, indicating no transference between oxygen and titanium [18]. All samples absorbed weakly in the visible region. The weak absorption in the visible region terminated at longer wavelength, with the onset of infrared absorption edge for all samples. At wavelengths above the absorption edge, adsorption bands occur. Strong absorption bands in this region may be associated with intervalence transitions [18–20].

In Fig. 8a, the TiO_2 films were prepared at oxygen flow rate of 3 sccm and different ion anode voltages. As the ion anode voltage increased, the absorption edge shifted towards longer wavelength, and a red-shift was observed. The TiO_2 films prepared at 120 eV exhibited a red-shift, suggesting that relatively large grains were contained [21–25]. In Fig. 8b, the TiO_2 films were prepared at an ion anode voltage of 110 eV and different oxygen flow rates. The absorption edge shifted towards longer wavelength as the oxygen flow rate increased. The red-shift may be attributed to the larger grain size [21–25].

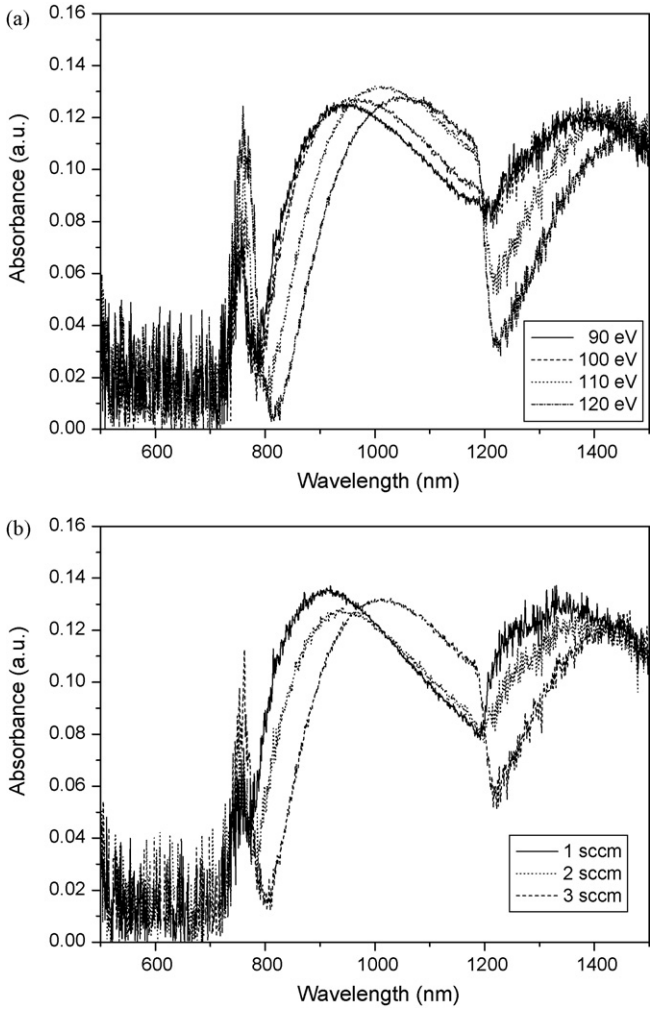

Fig. 8. The absorbance in the vis–IR region of TiO_2 films prepared at (a) different ion anode voltages and (b) different oxygen flow rates.

4. Conclusions

TiO_2 films with different properties, depending on experimental parameters, were deposited by ion beam assisted evaporation on PC substrates. The TiO_2 films are amorphous. Therefore, the linear refractive index was directly correlated with the porosity. The porosity decreased and the grain size increased as the ion anode voltage and the oxygen flow rate increased. The nonlinear refraction index of the TiO_2 film on the PC substrate was measured to be of the order of 10^{-8} cm^2 W^{-1} and the change in refractive index was of the order of 10^{-5}. As the ion anode voltage and oxygen flow rate increased, the transparent TiO_2 film showed a higher linear refractive index, a red-shift and obvious absorbance in the near-IR region. Therefore, TiO_2 film is a candidate for infrared optical application.

Acknowledgements

The authors would like to thank the Chienkuo Technology University for its mechanical support under the experiment and the National Science Council of the Republic of China, Taiwan, for financially supporting this research under Contract No. NSC-97-2221-E-260-004.

References

[1] Y. Djaoued, R. Bruning, D. Bersani, P.P. Lottici, S. Badilescu, Mater. Lett. 58 (2004) 2618.
[2] L. Sun, P. Hou, Thin Solid Films 455–456 (2004) 525.
[3] P.H. Giauque, H.B. Cherry, M.-A. Nicolet, Thin Solid Films 394 (2001) 136.
[4] E. György, E. Axente, I.N. Mihailescu, C. Ducu, H. Du, Appl. Surf. Sci. 252 (2006) 4578.
[5] S.F. Wang, Y.F. Hsu, Y.S. Lee, Ceram. Int. 32 (2006) 121.
[6] H.K. Jang, Y.S. Lee, T.K. Kim, J. Vac. Sci. Technol. A 18 (2000) 2932.
[7] J.D. Deloach, C.R. Aita, J. Vac. Sci. Technol. A 16 (1998) 1963.
[8] J.V. Grahn, M. Linder, E. Fredriksson, J. Vac. Sci. Technol. A 16 (1998) 2495.
[9] Y. Yasumi, U. Haruo, W. Shigeyuki, N. Hisakazu, Appl. Opt. 38 (1999) 6638.
[10] D. Mardare, A. Stancu, Mater. Res. Bull. 35 (2000) 2017.
[11] M.J. Soileau, W.E. Williams, N. Mansour, E.W. Van Stryland, Opt. Eng. 28 (1989) 1133.
[12] E.W.V. Stryland, Y.Y. Wu, D.J. Hagan, M.J. Soileau, K. Mansour, J. Opt. Soc. Am. B 5 (1988) 1980.
[13] M.J. Soileau, W.E. Williams, E.W. Van Stryland, IEEE J. Q. Elec. QE-19 (1983) 731.
[14] K. Mansour, M.J. Soileau, E.W. Van Stryland, J. Opt. Soc. Am. B 3 (1992) 1100.
[15] G.S. Vicente, A. Morales, M.T. Gutierrez, Thin Solid Films 391 (2001) 133.
[16] B.E. Yoldas, P.W. Partlow, Thin Solid Films 129 (1985) 1.

[17] W.D. Kingery, H.K. Bowen, D.R. Uhlmann, Introduction to Ceramics, Wiley, New York, 1976, p. 669.
[18] A.P. Roth, J.B. Webb, D.F. Williams, Solid State Commun. 39 (1981) 1269.
[19] H. Demiryont, K.E. Nietering, Sol. Energy Mater. 9 (1989) 79.
[20] H. Demiryont, L.R. Thomson, G.J. Collins, Appl. Opt. 25 (1986) 1311.
[21] D.H. Zhang, D.E. Brodie, Thin Solid Films 238 (1994) 95.
[22] K.H. Kim, K.C. Park, D.Y. Ma, J. Appl. Phys. 81 (12) (1997) 7764.
[23] S.S. Lin, J.L. Huang, Surf. Coat. Technol. 185 (2–3) (2004) 222.
[24] S.S. Lin, J.L. Huang, J. Mater. Res. 18 (2003) 1943.
[25] G.H. Li, L. Yang, Y.X. Jin, L.D. Zhang, Thin Solid Films 368 (2000) 163.